

Velocity scaling for optimizing replica exchange molecular dynamics

Maksim Kouza and Ulrich H. E. Hansmann

Citation: *J. Chem. Phys.* **134**, 044124 (2011); doi: 10.1063/1.3533236

View online: <http://dx.doi.org/10.1063/1.3533236>

View Table of Contents: <http://jcp.aip.org/resource/1/JCPSA6/v134/i4>

Published by the [AIP Publishing LLC](#).

Additional information on *J. Chem. Phys.*

Journal Homepage: <http://jcp.aip.org/>

Journal Information: http://jcp.aip.org/about/about_the_journal

Top downloads: http://jcp.aip.org/features/most_downloaded

Information for Authors: <http://jcp.aip.org/authors>

ADVERTISEMENT



Explore the **Most Cited**
Collection in Applied Physics

AIP
Publishing

Velocity scaling for optimizing replica exchange molecular dynamics

Maksim Kouza^{a)} and Ulrich H. E. Hansmann^{b)}

Department of Physics, Michigan Technological University, Houghton, Michigan 49931, USA

(Received 15 September 2010; accepted 9 December 2010; published online 27 January 2011)

We discuss the use of velocity rescaling for generating rejection-free exchange moves in replica exchange molecular dynamics. We test the efficiency of this approach for a common test case, the trp-cage protein. Advantages and limitations of the approach are discussed and possible extensions outlined. © 2011 American Institute of Physics. [doi:10.1063/1.3533236]

I. INTRODUCTION

The structure and function of proteins depend on a delicate interplay between genetic information (i.e., the sequence of amino acids that make up the protein chain) and environment (solvent and other proteins or other molecules). In many cases the energy landscape of a protein is more complex than traditional funnel theory suggests, and some of the involved processes may not be directly observable. In these more complex cases, computer simulations may still offer a way to a detailed understanding of folding and function of proteins.

Unfortunately, folding simulations are troubled by numerical difficulties. While optimized generalized-ensemble and replica exchange^{1–4} enhance the sampling of low-energy configurations,⁵ they have not yet solved the sampling problem. Particularly challenging are the simulations of proteins with explicit water. The necessarily large number of water molecules necessitates that the temperature intervals ΔT have to be chosen small. As a consequence, many replicas are required to cover the range between the lowest temperature (which is the one we are interested in) and the largest temperature. The latter is given by the highest relevant barrier in the system. The number n_R of round trips between the two extreme temperatures defines a lower bound on the number of independent configurations sampled at the target temperature. As the round trip times increases as \sqrt{M} with the number of replicas M , the number of independent sampled configurations decreases accordingly. Hence, protein simulations with explicit water require not only many replicas but also long simulation times in order to obtain sufficient statistics at temperatures of interest.

Various approaches have been proposed to speed up replica exchange simulations in general^{6–10} or specifically for the case of explicit solvent simulations of proteins.^{11,12} We have recently suggested to circumvent the above described problem of low acceptance rates and resulting large number of replicas through a rejection-free microcanonical replica exchange method.^{3,4} In the present paper, we extend this idea to proteins in the canonical ensemble which more closely resembles experimental settings. We test our approach for the trp-cage protein,^{13,14} a common model to test numerical methods.^{15,16} This protein has been previously investigated

with replica exchange methods^{17–20} by various groups,^{21,22} allowing a comparison with our results. In our simulations, the rejection-free replica exchange moves lead indeed to a faster flow along the temperature ladder. However, this faster flow does not translate into a more efficient sampling. Instead, it is more advantageous to combine rejection-free exchange moves with the standard exchange moves usually employed in replica exchange molecular dynamics.^{19,20}

II. METHODS

In canonical replica exchange^{17–19} two configurations with energies E_1 and E_2 are exchanged between temperatures T_1 and T_2 with probability $\exp(\Delta\beta\Delta E)$, with the inverse temperature given by $\beta = 1/k_B T$. These exchange moves generate for each replica a random walk in temperature that allows for escape out of local minima. Hence, the sampling becomes more efficient than by putting all computing resources in a single simulation at the lowest temperature.¹⁹

In a molecular dynamic simulation, the energy

$$E(x, v) = E_{\text{pot}}(x) + E_{\text{kin}}(v) \quad \text{with} \quad (1)$$

$$E_{\text{kin}}(v) = \frac{1}{2} \sum_i m_i v_i^2$$

is the sum of the potential energy E_{pot} , which depends only on the coordinates x , and the kinetic energy E_{kin} , which is solely a function of the velocities v . Scaling all velocities by a factor r changes the kinetic energy by

$$E_{\text{kin}}(rv) = r^2 E_{\text{kin}}(v). \quad (2)$$

In standard replica exchange molecular dynamics, this relation is used by scaling the velocities after a successful exchange with a factor

$$r_{(1,2)} = \sqrt{\frac{T_{(2,1)}}{T_{(1,2)}}}, \quad (3)$$

that depends on the temperatures T_1 and T_2 of the two replicas that are exchanged. The rescaling of the velocities leads to $v_{(1,2)}^{\text{new}} = v_{(2,1)}^{\text{old}}$, and therefore $\Delta E_{\text{kin}} = 0$. Hence, the probability for an exchange is given only by the difference of potential energies of the two replicas:

$$w(1 \leftrightarrow 2) = \exp(\Delta\beta\Delta E_{\text{pot}}). \quad (4)$$

^{a)}Electronic mail: mkouza@mtu.edu.

^{b)}Electronic mail: hansmann@mtu.edu.

In Refs. 3 and 4, we argued that microcanonical replica exchange simulations call for a different scaling. By definition of the ensemble, one has to assure that $\Delta E = 0$. Assuming $E_1 < E_2$ and scaling parameters r_1 and r_2 given by

$$\begin{aligned} r_{(1,2)} &= \sqrt{\frac{E_{(2,1)} - E_{\text{pot}}(\mathbf{x}_{1,2})}{E_{(1,2)} - E_{\text{pot}}(\mathbf{x}_{1,2})}} \\ &= \sqrt{\frac{E_{\text{kin}}(\mathbf{v}_{(2,1)}) \pm \Delta E_{\text{pot}}}{E_{\text{kin}}(\mathbf{v}_{1,2})}}, \end{aligned} \quad (5)$$

two configurations are exchanged with probability 1:

$$\begin{aligned} E_1(\mathbf{x}_1, \mathbf{v}_1) &= E_{\text{pot}}(\mathbf{x}_1) + E_{\text{kin}}(\mathbf{v}_1) \\ &= E_{\text{pot}}(\mathbf{x}_2) + r_2^2 E_{\text{kin}}(\mathbf{v}_2), \end{aligned} \quad (6)$$

$$\begin{aligned} E_2(\mathbf{x}_2, \mathbf{v}_2) &= E_{\text{pot}}(\mathbf{x}_2) + E_{\text{kin}}(\mathbf{v}_2) \\ &= E_{\text{pot}}(\mathbf{x}_1) + r_1^2 E_{\text{kin}}(\mathbf{v}_1). \end{aligned} \quad (7)$$

Such rejection-free moves are possible for $E_{\text{pot}}(\mathbf{x}_2) < E_1$, a restriction that does not violate detailed balance. Molecular dynamic time evolution between exchange moves ensures ergodicity. Hence, the sampling will lead for sufficiently long simulation times to the correct distribution

$$P(E_{\text{pot}}; E) \propto \Omega_{\text{pot}}(E_{\text{pot}}) E_{\text{kin}}^{n_f/2}, \quad (8)$$

where Ω is the density of states and n_f is the number of degrees of freedom.

The above scaling leading to rejection-free sampling has been used in Ref. 3 to study the trp-cage protein with an implicit solvent. However, this approach is not restricted to microcanonical simulations. Instead, it can be generalized to the more commonly used canonical ensemble without that the functional form of Eq. (5) changes. In the present paper, we test the efficiency of this approach in comparison with the standard replica exchange move.

Our test case is again the 20-residue trp-cage miniprotein (Protein Data Bank Identifier 1L2Y) which has become a commonly used test system for evaluation of new sampling schemes. The protein is simulated with the GROMACS program package²³ using the AMBER94 force-field²⁴ to describe the protein. Unlike in our previous work, we simulate the protein in an explicit solvent, the TIP3P water model.²⁵ AMBER94 is known to have a bias toward helical structures. While therefore extreme care is required when interpreting the results from simulations with this force-field, we regard its choice justified as the focus of the present work is on method development. The selection of AMBER94 and the TIP3 water model allows us to compare our results with previous work of Ref. 21. As these authors we use periodic boundary conditions and calculate the electrostatic interactions by the particle mesh Ewald method. The nonbonded interaction pair-lists are updated every 10 fs, using a cutoff of 1.2 nm. All bond lengths are constrained with the linear constraint solver LINCS (Ref. 26) as implemented in GROMACS, allowing us to integrate the equations of motion with a time step of 2 fs in the leap-frog algorithm.

The start configuration is generated by the LEAP program in the AMBER package, with the amino-acid sequence Ac-NLYIQWLKDGPPSSGRPPPS-NME as input. Methyl groups are added to the N- and C-termini, leading to a total of 313 atoms in the protein. This LEAP generated structure collapses in a short molecular dynamic run at $T = 400$ K into a compact (but unfolded) configuration that subsequently is solvated with 2645 water molecules in a cubic box of length 4.40 nm. In a final step, the whole system is minimized with the steepest decent method, before being equilibrated at 300 K with two successive molecular dynamic runs of 500 ps length each, the first one at constant volume and the second at constant pressure (1 atm).

The so-generated structure is the start configurations for our replica exchange simulation, with the 40 temperatures (280.0, 284.1, 288.2, 292.4, 296.7, 301.1, 305.6, 310.2, 314.9, 319.7, 324.6, 329.6, 334.7, 340.0, 345.4, 351.0, 356.6, 362.5, 368.4, 374.6, 380.9, 387.3, 394.0, 400.8, 407.8, 415.1, 422.5, 430.1, 438.0, 446.0, 454.3, 462.8, 471.6, 480.6, 489.8, 499.3, 509.0, 519.0, 529.2, and 539.7 K) taken from Ref. 21. The temperature of a given replica is controlled by a Nose–Hoover thermostat with a time coupling of $\tau_T = 0.5$ ps. Exchange attempts are made every 2 ps. Using two cores for each replica, we obtain an average speed of 5.6 ns/day on our cluster of Intel(R) Xeon(R) E5504 central processing units at 2.00 GHz. All our simulations run for a total of 100 ns.

When the all-atom simulations of the trp-cage relying on the GROMACS package proved to be time consuming, we chose instead a simple model, the Go-model of Ref. 27 as modified in Ref. 28. We follow the time evolution of the system by integrating the Langevin equation^{28,29} with a Verlet algorithm.³⁰ We choose a time step $\Delta t = 0.005\tau_L$, where we assume in the calculation of $\tau_L = (ma^2/\epsilon_H)^{1/2} \approx 3$ ps a typical value $m = 3 \times 10^{-25}$ kg (Ref. 31) and $a = 4$ Å. Setting $T_F = 0.58\epsilon_H$ we find with $T_F = 315$ K (Ref. 32) a value $\epsilon_H = 1.08$ kcal/mol. The reference structure is the first configuration in the NMR ensemble of the trp-cage protein as deposited in the Protein Data Bank under Identifier 1L2Y. Replica exchange simulations with this model are performed for eight temperatures in the range of 0.25–1.02 chosen such that the average acceptance ratio for standard exchange moves is $\approx 30\%$. Exchange attempts are made every 1000 time steps $\Delta t = 0.005\tau_L$. The system is equilibrated for a time $0.5 \times 10^5\tau_L$, and only afterward data are collected for another $2 \times 10^5\tau_L$.

III. RESULTS

Replica exchange is a way to enhance sampling of low-energy configurations in Monte Carlo or molecular dynamic simulations by allowing a replica to walk in temperature space between the target temperature T_1 and a temperature T_N that corresponds to the highest relevant barrier. We display in Fig. 1 such a walk in temperature space for one of the 40 replicas. Examples for both standard replica exchange molecular dynamics and for our rejection-free approach are presented. Through such a walk in temperature space a replica will find local minima (at low temperatures), but is also able to escape

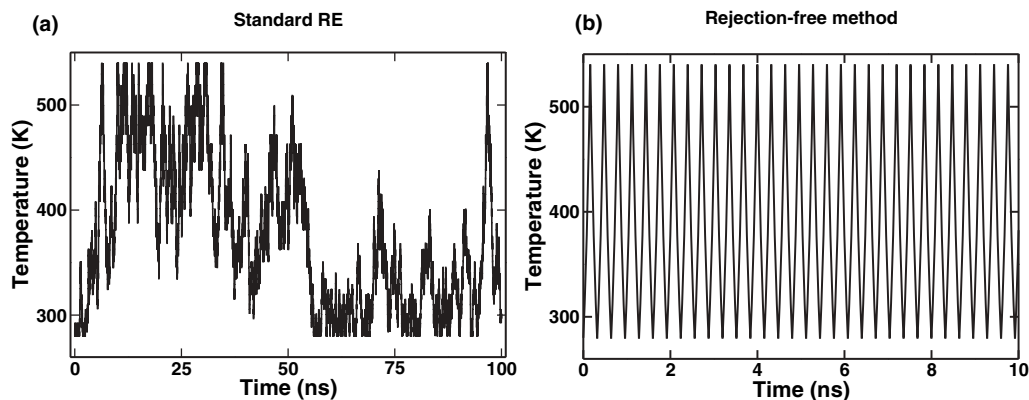


FIG. 1. Walk of a specific replica through temperature (a) in a standard canonical replica exchange molecular dynamic simulation and (b) with our rejection-free approach. Note that the large number of round trips observed for the later case required us to display only a short segment (10 ns) rather than the full 100 ns as in the case of standard replica exchange.

them (when at high temperatures). The number of round trips between T_1 and T_N and back is therefore a lower bound for the number of independent low-energy configurations sampled during a simulation. Within the displayed time span of 100 ns, standard replica exchange molecular dynamics leads to two round trips. Summing up all replicas we observe 79 round trips. This small number follows from the relatively large number of replicas required in explicit solvent protein simulations, see our discussion in Sec. I. On the other hand, with the rejection-free approach we observe within 10 ns already 30 round trips for a single replica. This suggests that the rejection-free approach leads to a more efficient sampling.

On a first look, this assumption seems to be supported by Fig. 2, where we plot the average potential energy as a function of temperature comparing standard replica exchange molecular dynamics and rejection-free replica exchange. The statistical error is smaller than the plot symbols, and the two curves are difficult to distinguish. However, the difference between both averages, displayed in the insets, is a decreasing function of temperature instead of fluctuating around zero. This systematic deviation indicates problems with the new approach. The existence of such problems is confirmed by

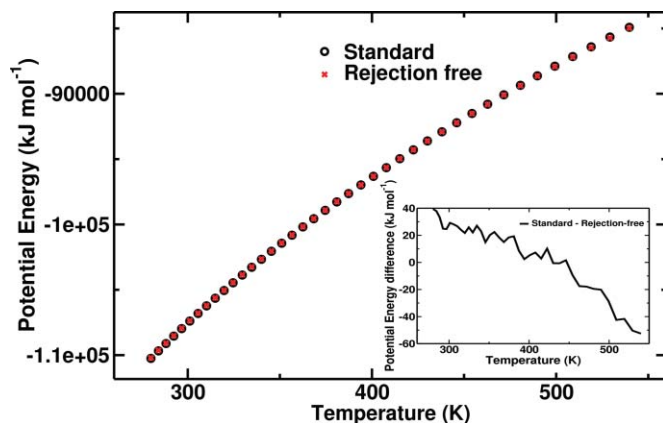


FIG. 2. Average potential energy (E_{pot}) as a function of temperature T for both standard canonical replica exchange molecular dynamics and our rejection-free variant. The inset displays the difference of both quantities as function of temperature.

Fig. 3, where we show for both approaches the distribution of root-mean-square deviation (RMSD) between sampled configurations and the experimentally determined ones (the first configuration of the NMR ensemble deposited in the Protein Data Bank under Identifier 1L2Y). The presented distributions are taken at $T = 280$ K. While in standard replica exchange molecular dynamics almost all sampled configurations are within 2 \AA to the NMR structure, we find a much broader distribution with rejection-free replica exchange.

This difference in distributions comes as a surprise, as rejection-free replica exchange molecular dynamics is formally correct. We attribute the problem to slow relaxation at the given temperatures after an exchange move. Only if relaxation at a given temperature is fast compared to the flow through temperature space, maximizing the flow (and therefore the number n_R of round trips) will lead to an enhanced sampling. This is not the case in the present simulation. In fact, increasing the time between replica exchanges (giving more time for relaxation) decreases the difference between the distributions (data not shown).

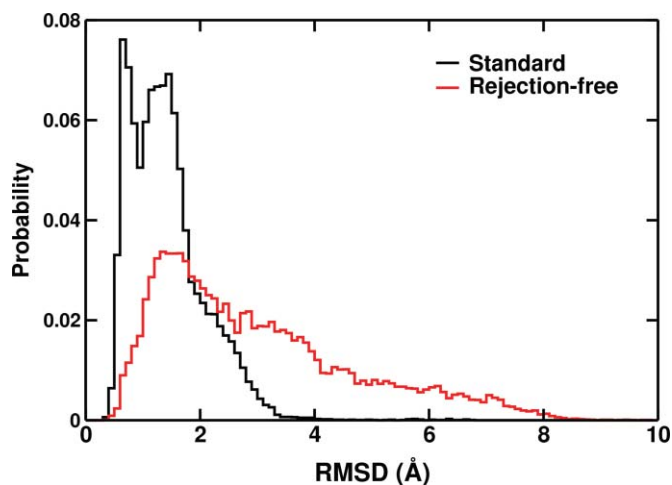


FIG. 3. Frequency P of configurations with a certain RMSD as observed at $T = 280$ K. Distributions are shown for both standard replica exchange molecular dynamics and simulations relying on the proposed rejection free exchange move.

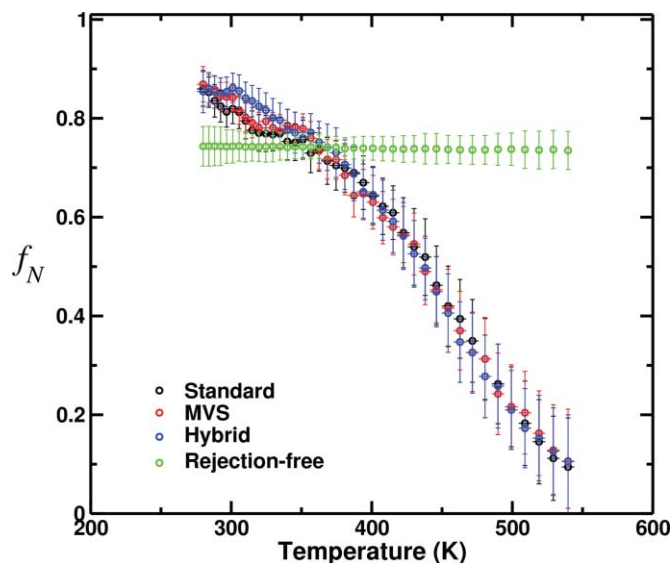


FIG. 4. Fraction f_n of nativelike configurations as a function of temperature. Displayed are the values obtained from standard replica exchange molecular dynamics, simulations using the rejection-free exchange move, such relying on the exchange move of Eq. (9) (marked MVS), and such as obtained with the hybrid method discussed in the text.

The net effect of the slow relaxation between the exchange moves is a lack of importance sampling. One can think of two approaches to overcome this problem. One is to combine the rejection-free move with the standard exchange move [using the scaling of Eqs. (4) and (3)] in a hybrid algorithm. The other approach is to replace the rejection-free exchange move by the scheme that we have proposed earlier in Ref. 3. Velocities are scaled as in Eq. (5), but an importance sampling is enforced by accepting exchange moves only with probability

$$w(i \leftrightarrow j) = \left(\frac{K_i^{\text{new}} K_j^{\text{new}}}{K_i^{\text{old}} K_j^{\text{old}}} \right)^{n_f/2}. \quad (9)$$

In this equation, K_i^{old} is the kinetic energy E_{kin} of the replica that sits *before* the exchange move at temperature T_i , K_i^{new} is the kinetic energy E_{kin} of the replica that sits *after* the exchange move at temperature T_i , and n_f marks the number of degrees of freedom of the system. As shown in Ref. 3, such importance sampling will lead to a distribution

$$P(E_{\text{pot}}) \propto \Omega(E_{\text{pot}}) E_{\text{kin}}^{n_f/2} \approx \Omega(E_{\text{pot}}) e^{-E_{\text{pot}}/k_B T}. \quad (10)$$

We have performed simulations of replica exchange using this approach, with same statistics as in the case of canonical replica exchange molecular dynamics and the rejection-free replica exchange. We display in Fig. 4 the fraction of folded states for these three approaches. Here, we define a configuration as folded if its RMSD to the NMR structure deposited in the Protein Data Bank is less than 2.2 Å. Both standard replica exchange molecular dynamics and the weighted approach lead to the same results, while the rejection-free replica exchange generates a different and nonphysical curve. Hence, exchanging replicas according to Eq. (9) leads to the correct distribution. However, it does not yield an improved sampling in terms of number of round

trips. In the case of standard replica exchange molecular dynamics, we measure 79 round trips within 100 ns (sum over all replicas). Exchanging replicas according to Eq. (9) results into 77 round trips over 100 ns. Hence, we conclude that both approaches are of similar efficiency.

While the replica exchange move of Eq. (9), depending only on the kinetic energies (instead of potential energies in the standard method), is interesting in itself and worthwhile to be explored further, for practical purposes more important may be another approach. In this hybrid method, one exchanges most of the times replicas according to Eq. (4), rescaling the velocities afterward by Eq. (3), but with a certain preset frequency the exchange is done with the rejection-free moves that follow from a velocity rescaling according to Eq. (5). In this way, one combines the shorter round trip times of rejection-free replica exchange with the importance sampling of the standard exchange move. As in the previous cases, we have tested this hybrid method in simulations of the trp-cage protein, using the same number of replicas and equal length (100 ns). In every 50th exchange attempt, the standard exchange probabilities of Eq. (4) are replaced by the rejection-free move following from velocity scaling according to Eq. (5). The fraction of nativelike configurations measure as obtained with this hybrid approach is also shown in Fig. 4. The measured values are consistent with the ones obtained by standard replica exchange molecular dynamics. This demonstrates that the hybrid approach generates indeed the correct distribution and therefore overcomes the lack of importance sampling in the rejection-free approach. However, unlike simulations relying on the exchange move of Eq. (9), the hybrid approach also leads to an increased number of round trips. Within 100 ns, 98 round trips are observed as opposed to only 79 round trips with standard replica exchange. This corresponds to an improvement by 24% which is significant in large scale simulations.

An interesting question is how the gain in efficiency depends on the mixing of standard and rejection-free exchange moves in the hybrid approach. A too small number of rejection-free moves will result in a diminishing gain over standard replica exchange, while too many such moves will cause the lack of importance sampling observed earlier. As the all-atom GROMACS simulations of the trp-cage protein are time consuming, we have investigated this question in simulations of a simpler model, the Go-model of Ref. 27. This model, modified in Ref. 28, has been successfully used in both single temperature^{33,34} and replica exchange molecular dynamics.³⁵ With this model we perform a series of hybrid replica exchange simulations where every N th exchange attempt is a rejection-free move with velocity scaling given by Eq. (5). The remaining $N - 1$ exchange attempts are accepted in the standard way with a probability given by Eq. (4), with the velocity rescaled according to Eq. (3). N varies from

TABLE I. The number n_R of round trips as a function of the frequency of rejection-free exchange moves. $N = 1$ corresponds to solely rejection-free moves, while $N = \infty$ marks the case of only standard exchange moves.

N	1	3	5	9	11	13	15	25	75	∞
n_R	1649	165	110	108	108	101	103	96	89	86

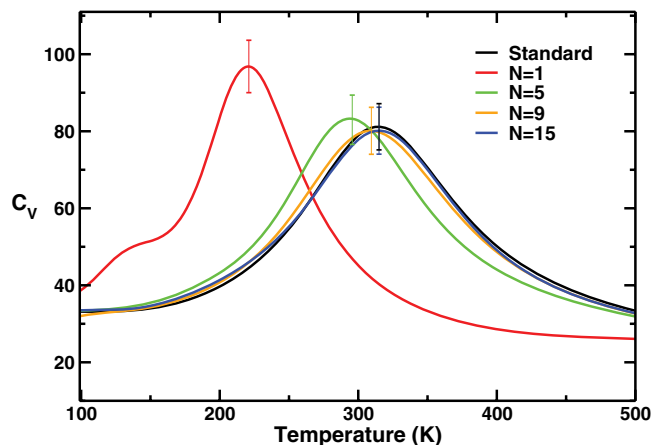


FIG. 5. The specific heat $C_V(T)$ as a function of temperature for various mixing ratios between standard and rejection-free moves. The data are taken from Go-model simulations as described in the text. The selected displayed error bars describe the typical variance of the data.

$N = 1$ (rejection-free approach) to $N = \infty$ (standard replica exchange). Table I lists the measured round trip times as function of N .

The listed results indicate that the number n_R of round trips drops quickly with increasing N approaching a “plateau” where n_R depends only weakly on N , before slowly converging to the value found in standard replica exchange molecular dynamics. Interestingly, the gain in sampling efficiency as measured by n_R is again of order 20%–30%. Figure 5 displays the specific heat C_V as a function of temperature for various values of N . Note the deviation between the curves obtained with standard replica exchange and the rejection-free approach ($N = 1$). With increasing N , the correct curve is quickly approached (at $\approx N = 9$). Note, however, that the differences of the C_V curves between standard replica exchange and hybrid method with small N are a function of simulation time. Figure 6 displays the curves for the case of $N = 5$ for different simulation times. With increasing length of simulations, the C_V curve of $N = 5$ approaches the one from standard replica exchange which is also plotted in the figure. This

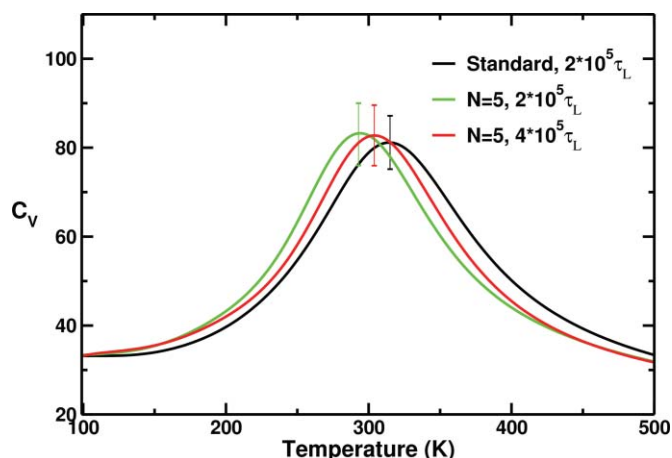


FIG. 6. The specific heat $C_V(T)$ as a function of temperature and length of simulation. The data are taken from Go-model simulations as described in the text. The selected displayed error bars describe the typical variance of the data.

reflects the lack of importance sampling observed in simulations with the rejection-free exchange move (that dominates for small N). Large simulation times will compensate for this lack.

IV. CONCLUSIONS

Unlike in Monte Carlo simulations where the velocity degrees of freedom are integrated out, molecular dynamics retains the velocity degrees of freedom. These additional degrees of freedom can be utilized in replica exchange simulations to optimize the flow of replicas through temperature space. In the present paper we have tested the efficiency of velocity rescaling in replica exchange molecular dynamics focusing on the case where it leads to rejection-free exchange moves. Such moves appear naturally in microcanonical replica exchange molecular dynamics and are tested here for a protein in the canonical ensemble, a more common experimental setting. As expected, such moves result in a much faster flow through temperature space. However, they do not yield a more efficient sampling. We discuss two variants that overcome this difficulty. The first one replaces the rejection-free exchange move by a weighted one that showed to be equivalent with the standard exchange move. More promising is the combination of rejection-free exchange moves with the traditional exchange moves usually employed in replica exchange molecular dynamics.^{19,20} A 20%–25% increase in round trip times (and therefore independent measurements) is observed and depends only weakly on the specific mixture of rejection-free and traditional moves. While this gain in efficiency is modest, it can be obtained with only little additional programming effort. We speculate that the improvement will be larger in systems with more pronounced bottlenecks in the energy landscape. Especially promising would be a test for polymer and protein aggregation,^{36,37} a problem that suffers from similar or even worse sampling difficulties than protein folding simulations.

We speculate that the velocity rescaling relation of Eq. (5) may also be useful in another hybrid approach where the potential energy E_{pot} is separated in two parts: $E_{\text{pot}}^{\text{ww}}$ that encompasses only interactions between water molecules and $E_{\text{pot}}^{\text{pw}}$ that is the sum of interactions between atoms within the protein and between protein and water. One can imagine rescaling of the velocities after an exchange move that compensates for the contributions of $E_{\text{pot}}^{\text{ww}}$, leading to an exchange of replicas with a probability $\exp(\Delta\beta\Delta E_{\text{pot}}^{\text{pw}})$ that depends only on protein–protein and protein–water interactions. As in hydrophobic-aided replica exchange method (HAREM) (Ref. 11) or solute tempering,¹² such a hybrid approach will allow a larger temperature spacing (and therefore simulations with smaller number of replicas) but potentially could avoid their convergence problems. We are testing this idea now in ongoing simulations.³⁸

ACKNOWLEDGMENTS

This work has been supported, in part, by the National Science Foundation (NSF) under research Grant

No. CHE-0809002. We thank Walter Nadler for discussions at an early stage of this work.

- ¹W. Nadler and U. H. E. Hansmann, *Phys. Rev. E* **75**, 026109 (2007).
- ²W. Nadler, J. H. Meinke, and U. H. E. Hansmann, *Phys. Rev. E* **78**, 061905 (2008).
- ³P. Kar, W. Nadler, and U. H. E. Hansmann, *Phys. Rev. E* **80**, 056703 (2009).
- ⁴W. Nadler and U. H. E. Hansmann, *Phys. Rev. E* **76**, 057102 (2007).
- ⁵O. Zimmermann and U. H. E. Hansmann, *Biochim. Biophys. Acta (BBA): Proteins and Proteomics* **1784**, 252 (2008).
- ⁶C. Zhang and J. Ma, *J. Chem. Phys.* **130**, 194112 (2009).
- ⁷E. Rosta, N.-V. Buchete, and G. Hummer, *J. Chem. Theory Comput.* **5**, 1393 (2009).
- ⁸J. Kim, T. Keyes, and J. E. Straub, *J. Chem. Phys.* **132**, 224107 (2010).
- ⁹D. J. Sindhikara, D. J. Emerson, and A. E. Roitberg, *J. Chem. Theory Comput.* **6**, 2804 (2010).
- ¹⁰D. M. Zuckerman and E. Lyman, *J. Chem. Theory Comput.* **2**, 1200 (2006).
- ¹¹P. Liu, X. Huang, R. Zhou, and B. J. Berne, *J. Phys. Chem. B* **110**, 19018 (2006).
- ¹²X. Huang, M. Hagen, B. Kim, R. A. Friesner, R. Zhou, and B. J. Berne, *J. Phys. Chem. B* **111**, 5405 (2007).
- ¹³J. W. Neidigh, R. M. Fesinmeyer, and N. H. Anderson, *Nat. Struct. Biol.* **9**, 425 (2002).
- ¹⁴C. Simmerling, B. Strockbine, and A. Roitberg, *J. Am. Chem. Soc.* **124**, 11258 (2002).
- ¹⁵A. Schug, T. Herges, and W. Wenzel, *Phys. Rev. Lett.* **91**, 158102 (2003).
- ¹⁶Y. He, Y. Xiao, A. Liwo, and H. A. Scheraga, *J. Comput. Chem.* **30**, 2127 (2009).
- ¹⁷C. J. Geyer and A. Thompson, *J. Am. Stat. Assoc.* **90**, 909 (1995).
- ¹⁸K. Hukushima and K. Nemoto, *J. Phys. Soc. Jpn.* **65**, 1604 (1996).
- ¹⁹U. H. E. Hansmann, *Chem. Phys. Lett.* **281**, 140 (1997).
- ²⁰Y. Sugita and Y. Okamoto, *Chem. Phys. Lett.* **314**, 141 (1999).
- ²¹D. Paschek, H. Nymeyer, and A. E. Garcia, *J. Struct. Biol.* **157**, 524 (2007).
- ²²A. Schug, W. Wenzel, and U. H. E. Hansmann, *J. Chem. Phys.* **122**, 194711 (2005).
- ²³B. Hess, C. Kutzner, D. van der Spoel, and E. Lindahl, *J. Chem. Theory Comput.* **4**, 435 (2008).
- ²⁴W. D. Cornell, P. Cieplak, C. I. Bayly, I. R. Gouls, D. M. Ferguson, D. C. Spellmeyer, T. Fox, J. W. Caldwell, and P. A. Kolman, *J. Am. Chem. Soc.* **117**, 5179 (1995).
- ²⁵W. L. Jorgensen, J. Chandrasekhar, J. D. Madura, R. W. Impey, and M. L. Klein, *J. Chem. Phys.* **79**, 926 (1983).
- ²⁶B. Hess, H. Bekker, H. J. C. Berendsen, and J. G. E. M. Fraaije, *J. Comput. Chem.* **18**, 1463 (1997).
- ²⁷C. Clementi, H. Nymeyer, and J. N. Onuchic, *J. Mol. Biol.* **298**, 937 (2000).
- ²⁸M. Kouza, C. F. Chang, S. Hayryan, T. H. Yu, M. S. Li, T. H. Huang, and C. K. Hu, *Biophys. J.* **89**, 3353 (2005).
- ²⁹M. P. Allen and D. J. Tildesley, *Computer Simulations of Liquids* (Oxford Science, Oxford, 1997).
- ³⁰W. C. Swope, H. C. Andersen, P. H. Berens, and K. R. Wilson, *J. Chem. Phys.* **76**, 637 (1982).
- ³¹T. Veitshans, D. Klimov, and D. Thirumalai, *Folding Des.* **2**, 1 (1997).
- ³²L. Qiu, S. A. Pabit, A. E. Roitberg, and S. J. J. Hagen, *J. Am. Chem. Soc.* **124**, 12952 (2002).
- ³³M. Kouza, M. S. Li, E. P. O'Brien, C. K. Hu, and D. Thirumalai, *J. Phys. Chem. A* **110**, 671 (2006).
- ³⁴M. S. Li and M. Kouza, *J. Chem. Phys.* **130**, 145102 (2009).
- ³⁵M. Kouza, C. K. Hu, and M. S. Li, *J. Chem. Phys.* **128**, 045103 (2008).
- ³⁶W.-J. Ma and C.-K. Hu, *J. Phys. Soc. Jpn.* **79**, 054001 (2010).
- ³⁷W.-J. Ma and C.-K. Hu, *J. Phys. Soc. Jpn.* **79**, 104002 (2010).
- ³⁸J. Z. Wang, G. H. Li, and U. H. E. Hansmann, *Velocity-scaling for Replica Exchange Simulations of Proteins in Explicit Solvent* (unpublished).